JOURNAL OF SOLID STATE CHEMISTRY 88, 94–103 (1990)

The Role of Disorder in Highly Correlated Metals and Insulators

T. F. ROSENBAUM* AND S. A. CARTER†

*The James Franck Institute and Departments of *Physics and †Chemistry, The University of Chicago, Chicago, Illinois 60637*

Received June 1, 1990

DEDICATED TO J. M. HONIG ON THE OCCASION OF HIS 65TH BIRTHDAY

We present measurements of the electrical resistivity at a series of hydrostatic pressures, the ac magnetic susceptibility, and the low temperature specific heat for single crystals of titanium-doped and vanadium-deficient V_2O_3 on both sides of the metal–insulator transition. We concentrate on the experimental signatures of disorder as a way to probe both correlation and charge localization effects. Comparison is made to previous $T \to 0$ results obtained for the rare earth oxide $La_{2-x}Sr_xCuO_4$ and the doped semiconductor Si : P in the immediate vicinity of the transition. © 1990 Academic Press, Inc.

Introduction

As emphasized in the classic papers of Mott (*1*) and Anderson (*2*), electron correlation and disorder are essential ingredients in the phenomenon of electron localization. Experimental studies of the metal–insulator transition have concentrated on two classes of materials, those where the electron–electron interactions appear to dominate and those where the effects of disorder seemingly drive the physics. As an example of the first class, consider vanadium sesquioxide, which undergoes a striking first order metal–insulator transition at a temperature $T_{MI} \sim 150$ K, marked by a jump in the electrical resistivity of seven orders of magnitude, a hysteresis loop of 10 to 12 K, a volume expansion of 1.4%, and antiferromagnetic ordering of the spins. Investigations (*3*) have centered on the remarkable electronic, magnetic, and structural behavior at the transition, which has served as a prototype for the physics of Mott–Hubbard transitions. In contrast to this discontinuous metal–insulator transition at finite temperature is the process of Anderson localization, whereby an insulator continuously evolves into a metal at zero temperature. Doped semiconductors are probably the simplest realization of this second class of materials, and they have been widely studied (*4*) to probe the nature of the metal–insulator transition in disordered systems. Experiments (*5*) have elucidated the critical behavior of the conductivity (in the metal) and the dielectric susceptibility (in the insulator) at absolute zero, as well as documenting the unusual low temperature corrections to transport processes due to the effects of the random distribution of the charge donors.

The division of real systems into two separate categories, one represented by the physics of disorder, the other denoted as highly correlated, is necessarily artificial. For example, electrons in a sufficiently disordered metal at low temperature do not travel anymore as Bloch waves, but ran-

0022-4596/90 $3.00

domly walk their way through the material. Hence, increasing the disorder similarly increases the importance of Coulomb effects as the electrons diffuse more slowly and interact more strongly. Moreover, the magnetic character of disordered electronic systems appears to be intertwined with their critical behavior at the metal–insulator transition. Various magnetic (*6*) measurements on barely metallic Si : P at milliKelvin temperatures indicate the presence of localized spins above the transition. It appears likely that a theory incorporating localization, electron interactions, and the spin degrees of freedom will be required to account for the full spectrum of electronic, magnetic, and dielectric behavior of disordered materials in the vicinity of the Anderson transition.

It is the thesis of this paper that the effects of disorder equally well need to be incorporated in a full description of Mott–Hubbard transitions. In particular, as T_{MI} is driven down in temperature by internal chemical (e.g., via alloying) or external applied pressure, the quantum nature of the localization process must become germane. The metal–insulator transition itself may be modified by it. At a minimum, we can use the diagnostic tools developed in milliKelvin temperature studies of doped semiconductors and amorphous alloys to help understand the fundamental low temperature character of highly correlated metals and insulators.

We divide this article into discussions of The Disordered Insulator, The Disordered Metal, and Correlations and Disorder at the Transition. We present preliminary results (*7*) on titanium-doped and vanadium-deficient V_2O_3 as well as low temperature studies (*8*) of (insulating) $La_{2-x}Sr_xCuO_4$, both in the context of what we have learned from earlier experiments (*9*) on the prototypical disordered system, Si : P. In addition, we attempt to outline new experiments which bear on the fundamental physics in the vicinity of the metal–insulator transition.

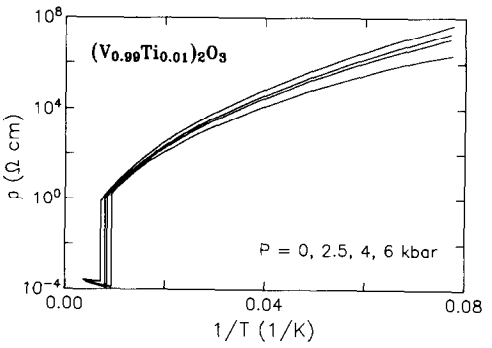

FIG. 1. Resistivity, ρ, as a function of inverse temperature, $1/T$, at a series of hydrostatic pressures, P, for a single crystal of Ti-doped V_2O_3 on cooling. A simple, activated form, representing the opening of the insulating gap, is only appropriate over a narrow range of T just below the metal–insulator transition temperature, $T_{MI}(P)$.

The Disordered Insulator

We plot in Fig. 1 the c-axis resistivity, ρ, as a function of inverse temperature, $1/T$, at a series of hydrostatic pressures, P, for a single crystal of $(V_{0.99}Ti_{0.01})_2O_3$ grown at Purdue. Metallic behavior at high T is abruptly interrupted by a jump in ρ of order four decades, marking the transition into the insulator. Pressure applied via a standard BeCu cell (using silicone oil as the hydrostatic pressure medium) helped maintain the electrical contacts through the volume expansion at the transition and permitted data collection for temperatures well below T_{MI}. All curves shown are for the cooling cycle only.

The metal–insulator transition temperature, T_{MI}, is depressed smoothly with increasing P, as expected (*3*). At no pressure, however, is a simple activated form appropriate for the resistivity in the insulator over more than a narrow range close to T_{MI}. The form $\rho(T) = \rho_0 \exp(\Delta/T)$ represents the opening of the insulating (Mott–Hubbard and/or Slater) gap, but it is clear from the curvature of ρ vs $1/T$ in Fig. 1 that slower than exponential conduction processes pre-

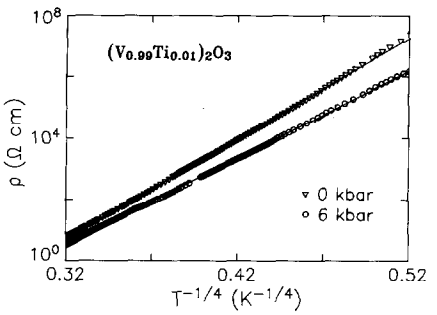

FIG. 2. Logarithm of the low temperature ($13 \leq T \leq 95$ K) insulating resistivity from the previous figure vs $T^{-1/4}$, fit to a Mott variable range hopping form (solid lines) at the pressure extremes of our experiment.

vail at low temperature. A stretched exponential form for the resistivity, $\rho(T) = \rho_1 \exp(T_0/T)^{\beta}$, with $0 < \beta < 1$, is a characteristic way to account for the effects of disorder on the insulating state in the low T limit. Mott variable range hopping (*10*) corresponds to $\beta = 1/(d + 1)$, where d is the system dimensionality. There is not enough thermal energy to excite electrons across the gap, so charge transport occurs by phonon-assisted hopping to states far away in space, but close by in energy.

We plot in Fig. 2 $\log \rho$ vs $(1/T)^{1/4}$ for the Ti-doped sample of V_2O_3 at the lowest and highest pressures for T well below T_{MI}. The solid lines are fits of the data to three-dimensional variable range hopping. We find that the characteristic energy for the hopping state, T_0, systematically decreases with increasing P. It must go to zero at sufficiently high pressure, where the metallic phase is stabilized at all T. We can estimate a localization length, α^{-1}, via the relation (*10*) $\alpha^{-1} \approx [kT_0N(E_F)/16]^{1/3}$, where $N(E_F)$ is the density of states at the Fermi level and k is Boltzmann's constant. Assuming a $N(E_F)$ of 1 state per vanadium atom (*11*), we find $\alpha^{-1} = 0.6$ Å for $P = 0$. Although T_0 is almost halved by $P = 6$ kbar, the localization length only increases by 20% because of the cube root dependence.

When electron–electron interactions in the presence of disorder are sufficiently strong, a soft gap is opened in the density of states. Variable range hopping conduction with this so-called Coulomb gap (*12*) also gives a stretched exponential form for the resistivity, but with $\beta = 1/2$ (for both two- and three-dimensional systems). Here, $\alpha^{-1} \approx e^2/kT_0\kappa$, where e is the charge of the electron and κ is the dc dielectric constant of the material. Hence, observation of Coulomb gap behavior can provide a quantitative measurement of an insulator's dielectric character.

We show Coulomb gap behavior at low temperature in the rare earth oxide $La_{1.98}Sr_{0.02}CuO_4$ in the left-hand panel of Fig. 3. From the value of T_0 (the slope of $\log \rho$ vs $T^{-1/2}$), we estimate (*8*) $\kappa \geq 100$, in support of contentions that high temperature superconductivity evolves with doping from an insulating state on the verge of a ferroelectric instability. At higher Sr concentration, we find Mott variable range hopping with $\beta = 1/4$, as evidenced by the behavior of $La_{1.95}Sr_{0.05}CuO_4$ for $0.05 \leq T \leq 3.0$ K (right-hand panel, Fig. 3). We interpret the change in β as an indication that at

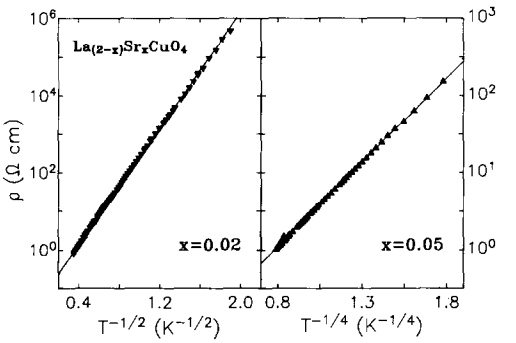

FIG. 3. As a function of Sr concentration, the logarithm of the low-temperature resistivity in the insulator crosses over from a $T^{-1/2}$ to $T^{-1/4}$ dependence, indicating variable range hopping conduction in the presence of carrier interactions (Coulomb gap behavior) and in the case of sufficiently screened interactions, respectively. Following Ref. (*8*).

the higher doping level the hole concentration has increased sufficiently to provide screening of the Coulomb gap even to the lowest temperatures measured. If it were possible to measure closer to $T = 0$, at higher resistivities, we would expect a crossover to the Efros–Shklovskii form, $\rho \propto \exp(T_0/T)^{1/2}$.

Although strong electron–electron interactions are essential to the physics of the Mott–Hubbard insulator, we do not observe the opening of a Coulomb gap at low T in $(V_{0.99}Ti_{0.01})_2O_3$. It may be that we simply have not extended our measurements (limited by the resistance exceeding 10^{11} Ω) to low enough temperatures. It may also be that the on-site Coulomb repulsion, as parameterized by the Hubbard U, modifies the spectrum of available hopping states and/or the nature of the screening. We note that the hard Hubbard gap and the soft Coulomb gap are not related directly, the former owing its existence primarily to intraatomic repulsion while the latter depends on the long-range interatomic electron–electron interaction which is screened at high temperature. Nonetheless, understanding the relationship between the two may provide new insights into the nature of the correlations in the insulating state.

Not all disorder is the same. We compare in Fig. 4 the low temperature heat capacity of titanium-doped and vanadium-deficient V_2O_3, less a fitted Schottky tail from the vanadium hyperfine interaction. The samples have approximately the same metal-insulator transition temperature, and T_{MI} is depressed identically in the two cases with the application of hydrostatic pressure (*7*). Yet, in the plot of C/T vs T^2, the single crystals of $(V_{0.99}Ti_{0.01})_2O_3$ and $V_{1.9967}O_3$ have different slopes as well as different $T = 0$ intercepts. Here, the slope gives the sum of the phonon and magnon contributions to the specific heat, while any non-zero intercept reflects the presence of two-level systems due to disorder in the insulator.

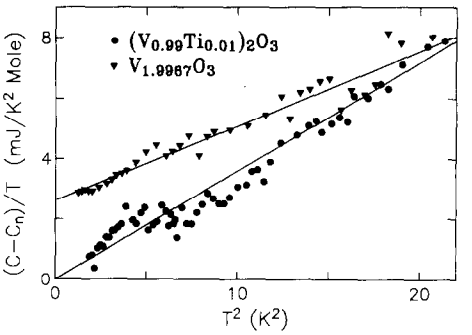

FIG. 4. Specific heat, C, less the nuclear Schottky contribution, $C_n \propto 1/T^2$. Lines are least square fits to a T^3 lattice and magnon term plus a linear T term due to disorder. Only the vanadium-deficient sample shows evidence for a significant density of two-level systems.

In the standard model (*13*) for the linear T term in the specific heat due to disorder, $C = 2n_0k^2T \int x^2\mathrm{sech}^2x dx$, where k is Boltzmann's constant and n_0 is the density of two-level systems, usually expressed in units of $J^{-1}m^{-3}$. For $V_{1.9967}O_3$ we have $n_0 = 2.2 \times 10^{47} J^{-1}m^{-3}$. In comparison (*14*), a structural glass like SiO_2 has $n_0 = 8.4 \times 10^{45} J^{-1}m^{-3}$, while the metglass $Zr_{0.7}Pd_{0.3}$ has $n_0 = 2.7 \times 10^{46} J^{-1}m^{-3}$. We believe that the vanadium vacancies in metal-deficient V_2O_3 provide multiple sites for oxygen reorientations, which leads to the large number of two-level systems. These modes might also provide extra states in the gap, which could influence strongly the low temperature hopping conduction.

The Disordered Metal

Our start for the study of the highly correlated metal is with a just insulating sample of vanadium-deficient V_2O_3! We show in Fig. 5 the characteristic behavior of the resistivity and the ac magnetic susceptibility at the metal-insulator transition for an oriented single crystal of $V_{1.987}O_3$, including the discontinuous jump at T_{MI} and the hysteresis loop on cooling and warming. The resistivity

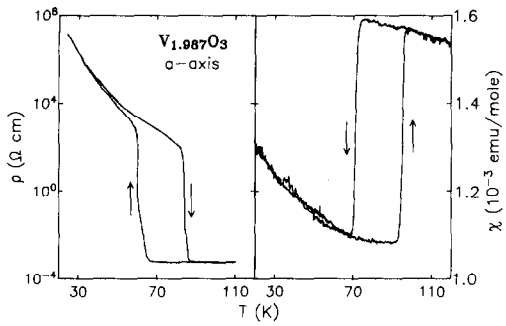

FIG. 5. The electronic and magnetic discontinuities at the finite temperature metal–insulator transition in a single crystal of nonstoichiometric V_2O_3. Hysteresis loops are shown in both the resistivity, ρ, and ac magnetic susceptibility, χ.

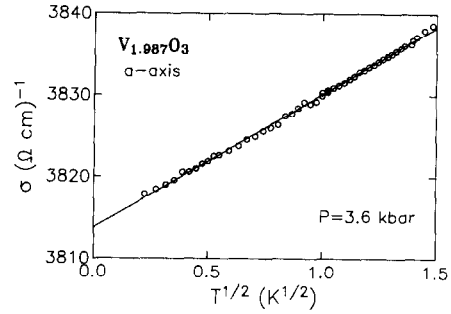

FIG. 7. The low temperature portion of the previous figure plotted as conductivity, σ, vs $T^{1/2}$. The square-root temperature dependence is characteristic of diffusive transport in the metal due to electron–electron interactions in the presence of disorder.

measurements are actually at a small pressure (~1/4 kbar) in order to maintain electrical contact at low temperature, which accounts for the small depression of T_{MI} relative to the ambient pressure susceptibility jump from antiferromagnet to paramagnet. Data for the c-axis is identical except for a small difference in scale.

The disordered $V_{1.987}O_3$ is close enough to the boundary where the metallic phase is stabilized at all T that we can push it across with only a small amount of hydrostatic pressure. We plot in Fig. 6 $\rho(T)$ for this

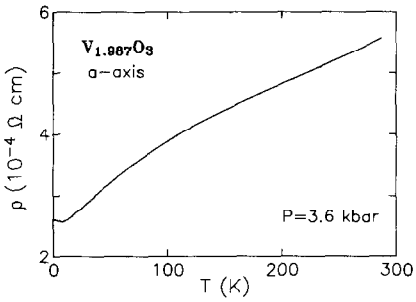

FIG. 6. Resistivity, ρ, as a function of temperature, T, for the vanadium-deficient crystal of V_2O_3 shown in Fig. 5, but pushed through the insulator–metal transition with the application of 3.6 kbar of hydrostatic pressure, P. The various transport regimes are described in the text.

sample at $P = 3.6$ kbar. The sample is metallic (and nonsuperconducting) down to at least $T = 20$ mK. At highest temperatures, the resistivity is effectively linear in T. At lower temperature, there is a crossover in ρ to a superlinear temperature dependence, which is cut off at low T by a resistivity minimum associated with the antiferromagnetic ordering of the spins. In this region, the resistivity approaches a T^2 form, reflecting enhanced electron–electron interactions and usually analyzed within a Brinkman–Rice (*15*) framework for the correlated metal. At the lowest temperatures, $\rho \propto T^{1/2}$, a form unheard of for crystalline systems but characteristic of electron–electron interactions in the presence of disorder (*5*, *16*). We demonstrate in Fig. 7 the $T^{1/2}$ dependence of the conductivity, σ, for our single crystal of $V_{1.987}O_3$ at $P = 3.6$ kbar over the temperature range $0.05 \leq T \leq 2.2$ K.

In addition to underlining the sensitive role of disorder at low T in the highly correlated metal, the square-root temperature dependence of the electrical transport provides us with a new mechanism to quantitatively assess the salient physical characteristics of the interaction-dominated metal. We turn to experience with the doped semiconductor Si : P to illustrate this point.

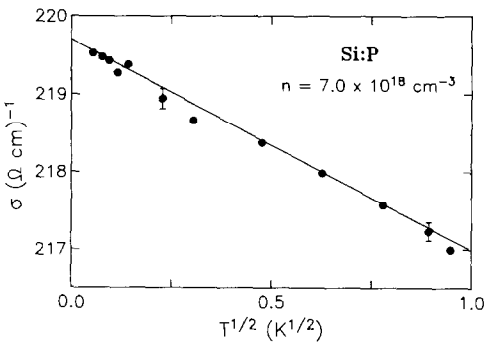

FIG. 8. The low temperature conductivity, σ, vs $T^{1/2}$ for a degenerately doped single crystal of Si : P. Following Ref. (*9*).

Phosphorus doped silicon is a well-characterized, homogeneous system where P donors sit substitutionally and randomly in a dislocation-free Si lattice. The outer electron of the shallow donor moves with a large effective Bohr radius which encompasses many lattice sites. At low temperature, the discreteness of the lattice is unimportant and the donor electrons move in the random potential of the impurity (donor) sites. When degenerately doped, the donors are in extended states, but close to the metal–insulator transition their motion is diffusive and electron–electron interactions cannot be ignored. In fact, the lowest temperature correction to the $T = 0$ conductivity is due to electron–electron interactions in the presence of disorder, giving the unusual cusp-like behavior: $\sigma(T) = \sigma(0) + mT^{1/2}$. We graph in Fig. 8, σ vs $T^{1/2}$ down to $T = 3$ mK for a single crystal of Si : P with donor density $n = 7.0 \times 10^{18}\,\mathrm{cm}^{-3}$, nearly a factor of two above the critical density for the metal–insulator transition.

Calculations (*5, 17*) considering Coulomb interactions with electron–electron scattering modulated by random impurities give $\sigma(T) = \sigma(0) + \alpha(4/3 - \lambda F)T^{1/2}$, where $\lambda = 2$ for a single isotropic valley, but because of anisotropy factors $\lambda = 4$ for Si : P. In both cases, $\alpha = [T_F(m^*D/\hbar)]^{-1/2}$, where T_F is the Fermi temperature, m^* is the effective mass, and D is the diffusion constant. The dimensionless term F is a function of $X \equiv (2k_F/K)^2$ and it results from the Hartree interaction, where k_F is the Fermi wavevector and K is the screening wavevector. It is given by $F = \ln[(1 + X)/X]$ and ranges from 0 to 1. Far above the transition, at high carrier density, X is large and $F \to 0$. This produces a positive value for the slope of the $T^{1/2}$ term, m, in some systems (e.g., $V_{1.987}O_3$, Fig. 7). Closer to the transition, where most of the Si : P data is taken, $X \leq 1$ and $\lambda F > 4/3$, yielding negative values of m. Very close to the critical density for the transition, n_c, the screening breaks down, K may become small, and $F \to 0$ again, causing m to change sign. We show in Fig. 9 the variation of m with n for a series of Si : P samples. The solid line is calculated from the equations above, but scaled by a numerical factor. Hence, the magnitude of m as well as its dependence on carrier density is a measure of not only the diffusion constant D, but of the Hartree interaction and the screening wavevector as the transition is approached from above.

The magnetic field dependence of the $T \to 0$ conductivity can provide additional information about correlations in the presence of disorder. Lee and Ramakrishnan (*18*) have shown that for the interaction model in the limit of $m_eD/\hbar \gg 1$, where m_e is the bare mass of the electron, a positive magnetoresistance of the form $H^{1/2}$ is produced due to the spin splitting of electrons with opposite spin. The energy splitting is of the usual form, $g\mu_B H$. In the high-field limit,

$$\rho(H,T) = \rho(0,0) - \alpha\rho^2(0,0)\left(\frac{4}{3} - \lambda F\right)T^{1/2} + 0.77\alpha\rho^2(0,0)F(g\mu_B/k)^{1/2}H^{1/2},$$

an expression which involves (and can constrain) some of the same physical quantities essential to understanding $\sigma(T)$.

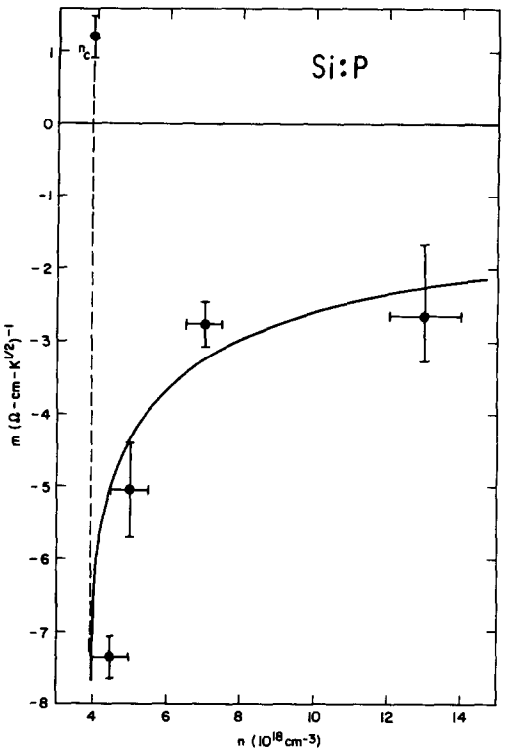

FIG. 9. The slope, m, of the $T^{1/2}$ term in the $T \to 0$ conductivity as a function of donor density, n, for metallic samples of Si : P. m becomes large and negative as the critical density for the metal–insulator transition, n_c, is approached per the equations in the text (solid line). Very close to n_c screening breaks down causing m to change sign (the dashed line is a guide to the eye). Following Ref. (9).

The important features of this equation are demonstrated in Fig. 10, which shows $\rho(H,T)$ plotted against $H^{1/2}$ at four temperatures for a sample of Si : P with $n = 3.84 \times 10^{18}$ cm^{-3}. This sample is only 3% above the transition, but its zero-temperature conductivity is still twice that of Mott's characteristic ("minimum metallic") conductivity, σ_M. The solid lines are best fits to the data and show the $H^{1/2}$ dependence above 300 Oe. The slopes for the four temperatures are nearly the same, in agreement with theory. The extensions of these straight lines to $H^{1/2} \to 0$ provide values of ρ which should be linear in $T^{1/2}$ as shown by the expression for $\rho(H,T)$. This plot is shown in the inset to Fig. 10. At $H = 0$ the resistivity becomes

$$\rho(0,T) = \rho(0,0) - \alpha\rho^2(0,0)\left(\frac{4}{3} - \lambda F\right) T^{1/2},$$

and this $T^{1/2}$ dependence is also shown in the inset, where both curves are constrained to go through the same value of $\rho(0,0)$. This type of analysis provides a way to include the effects of the spin degrees of freedom on the diffusive motion of the correlated electrons. The extension to substitutionally doped or vanadium-deficient V_2O_3 is complicated, however, by the antiferromagnetic ordering of the spins below $T \approx 10$ K in the metal.

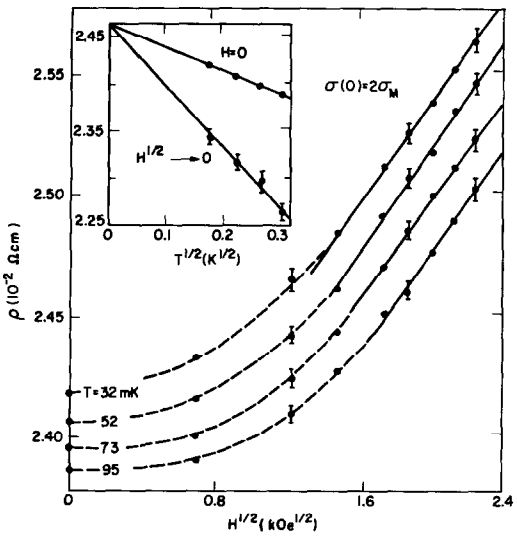

FIG. 10. Resistivity, ρ, vs $H^{1/2}$ at four temperatures, T, for a single crystal of Si : P with $n \approx 1.03n_c$. At high fields ρ is proportional to $H^{1/2}$ with a slope independent of T, in agreement with equations in the text. The intercepts of the solid lines, as well as ρ measured in zero field, are proportional to $T^{1/2}$ (inset), indicating the importance of correlations modulated by disorder. From Ref. (9).

Correlations and Disorder at the Transition

The finite temperature metal–insulator transition in V_2O_3 involves not only a discontinuous electronic transition, but accompanying magnetic and structural changes. In the $T \rightarrow 0$ limit, the situation becomes less complex. We sketch in Fig. 11 a simplified phase diagram (*19*) for titanium-doped, vanadium-deficient, and/or compressed vanadium sesquioxide. Here, we parameterize the internal chemical pressure and/or the external applied pressure by the ratio B/U, where B is the bandwidth and U is the intraatomic Coulomb repulsion.

Note that the $T = 0$ metal–insulator transition does not need to be linked with a magnetic transition; it is from antiferromagnetic metal to antiferromagnetic insulator, in contradistinction to the usual Mott–Hubbard finite temperature paramagnetic metal to antiferromagnetic insulator transition. We plot in Fig. 12 the ambient pressure ac magnetic susceptibility vs temperature for a barely metallic (at all T) oriented single crystal of $V_{1.982}O_3$ in order to illustrate the low T magnetic transition in the metal. The contrasting behavior of the a- and c-axis susceptibility is a classic example of the different magnetic response along the easy and hard axes of an antiferromagnet.

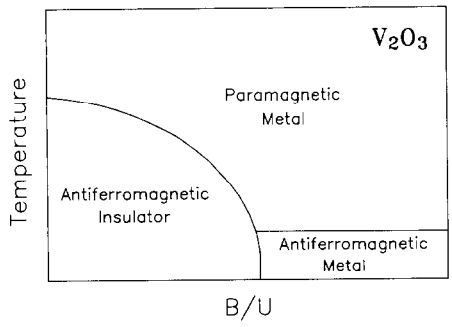

FIG. 11. Generalized phase diagram for V_2O_3. Ti-doping, vanadium deficiency, and hydrostatic pressure are all parameterized in terms of the ratio of the bandwidth to the Coulomb intraatomic repulsion, B/U.

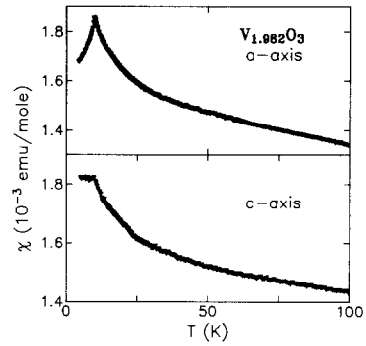

FIG. 12. The ac magnetic susceptibility, χ, of an oriented single crystal of vanadium-deficient V_2O_3 showing the transition along both the hard and easy axes from paramagnetic to antiferromagnetic metal at temperature $T \sim 10$ K.

We also know from the discussion in the previous two sections that the effects of disorder are prevalent at low temperature on both sides of the metal–insulator transition. In light of these observations, the question arises as to whether the $T = 0$ transition is still of the Mott–Hubbard-type. Sufficient disorder will, at a minimum, modify the traditional description and, in the extreme, will convert it to a continuous Anderson-type transition (*20*). Measurements of the $T \rightarrow 0$ critical behavior of the conductivity in the metal and the dielectric susceptibility in the insulator as a function of doping or pressure should shed light on this issue. Moreover, the interplay of electron correlations and localization effects at the metal–insulator transition may differ with the type of disorder introduced. For example, vanadium-deficient V_2O_3 with its large concentration of two-level systems is probably more likely to be in the Anderson limit than its substitutionally-doped analog.

A question remains as to the role of the magnetic degrees of freedom. We might expect the possibility of an enhancement with increasing disorder of the Wilson ratio, the ratio of the spin susceptibility to the specific heat. Recent results (*21*) on barely metallic

Si : P down to milliKelvin temperatures indicate a Wilson ratio considerably larger than can be expected in either the Brinkman–Rice or interaction–disorder scaling theory models (*22*) of the metal–insulator transition, and are interpreted as evidence for the presence of localized spins. Hence, a dependence of the Wilson ratio in V_2O_3 on alloying or perhaps even radiation damage would provide a powerful key to understanding the part played by the magnetic character of highly correlated, disordered electronic systems.

Conclusions

Vanadium sesquioxide has served as a prototype for the study of the physics of the Mott–Hubbard transition. With substitutionally doped and metal-deficient single crystals, we find the hallmark signatures of disorder in experiments at low temperature. These include variable range hopping conduction and large two-level system contributions to the specific heat in the insulator, as well as a sublinear temperature dependence of the conductivity due to diffusive transport in the metal. We analyze these effects of disorder with regard to previous investigations on rare earth oxides and doped semiconductors. Our results raise new questions about the ground state properties of highly correlated insulators and metals in the presence of disorder, and even about the nature of the $T \rightarrow 0$ metal–insulator transition itself. Quantitative analysis of the effects of disorder may provide new avenues of approach to understanding the relative roles and interplay of electron–electron interactions and electron localization effects.

Acknowledgments

We are indebted to J. M. Honig and J. Spalek for teaching us about the intricacy and beauty of the vanadium sesquioxide system. The experimental work reported here could not have been completed without the help of J. Yang. We are also grateful to P. Metcalf for reannealing the V_2O_3 crystals used in this research. The work at The University of Chicago was supported by NSF DMR 8816817.

References

1. N. F. MOTT, *Proc. Cambridge Philos. Soc.* **32,** 281 (1949); N. F. MOTT, *Proc. Phys. Soc. London A* **62,** 416 (1956).
2. P. W. ANDERSON, *Phys. Rev.* **109,** 1492 (1958).
3. For reviews see D. B. MCWHAN, A. MENTH, AND J. P. REMEIKA, *J. Phys. (Paris)* **32(C1),** 1079 (1971); S. A. SHIVASHANKAR AND J. M. HONIG, Phys. Rev. B **28,** 5695 (1983); N. F. MOTT, "Metal–Insulator Transitions," Taylor & Francis, London (1974).
4. See, for example, R. F. MILLIGAN, T. F. ROSENBAUM, G. A. THOMAS, AND R. N. BHATT, *in* "Electron–Electron Interactions in Disordered Systems" (A. L. Efros and M. Pollak, Eds.), p. 231, North-Holland, Amsterdam (1985).
5. For a recent review, see P. A. LEE AND T. V. RAMAKRISHNAN, *Rev. Mod. Phys.* **57,** 287 (1985).
6. See, for example, M. A. PAALANEN, S. SACHDEV, R. N. BHATT, AND A. E. RUCKENSTEIN, *Phys. Rev. Lett.* **57,** 2061 (1986); H. ALLOUL AND P. DELLOUVE, *Phys. Rev. Lett.* **59,** 578 (1987); R. N. BHATT, *Phys. Scr. T* **14,** 7 (1986).
7. S. A. CARTER, J. YANG, T. F. ROSENBAUM, J. SPALEK, AND J. M. HONIG, to be published.
8. B. ELLMAN, H. M. JAEGER, D. P. KATZ, T. F. ROSENBAUM, A. S. COOPER, AND G. P. ESPINOSA, *Phys. Rev. B* **39,** 9012 (1989).
9. T. F. ROSENBAUM, R. F. MILLIGAN, M. A. PAALANEN, G. A. THOMAS, R. N. BHATT, AND W. LIN, *Phys. Rev. B* **27,** 7509 (1983), and extensive references therein.
10. N. F. MOTT, *Philos. Mag.* **19,** 635 (1969); N. F. MOTT AND E. A. DAVIS, "Electronic Processes in Non-Crystalline Materials," 2nd ed., Oxford Univ. Press, London (1979).
11. C. CASTELLANI, C. R. NATOLI, AND J. RANNINGER, *J. Phys. (Paris)* **37(C4),** 199 (1976).
12. A. L. EFROS AND B. I. SHKLOVSKII, *J. Phys. C* **8,** L49 (1979).
13. P. W. ANDERSON, B. I. HALPERIN, AND C. M. VARMA, *Philos. Mag.* **25,** 1 (1972); W. A. PHILLIPS, *J. Low Temp. Phys.* **7,** 351 (1972).
14. R. O. POHL, *in* "Amorphous Solids: Low Temperature Properties" (W. A. Phillips, Ed.), p. 27, Springer-Verlag, Berlin (1981).
15. W. F. BRINKMAN AND T. M. RICE, *Phys. Rev. B* **2,** 4302 (1970).
16. T. F. ROSENBAUM, K. ANDRES, G. A. THOMAS, AND P. A. LEE, *Phys. Rev. Lett.* **46,** 568 (1981).

17. B. L. ALTSHULER, A. G. ARONOV, AND P. A. LEE, *Phys. Rev. Lett.* **44,** 1288 (1980); B. L. ALTSHULER, D. KHEMELNITZKII, A. I. LARKIN, AND P. A. LEE, *Phys. Rev. B* **22,** 5142 (1980).
18. P. A. LEE AND T. V. RAMAKRISHNAN, *Phys. Rev. B* **26,** 4009 (1982).
19. J. SPALEK, A. DATTA, AND J. M. HONIG, *Phys. Rev. Lett.* **59,** 728 (1987) provide a rationalization of the full phase diagram for pure and doped V_2O_3 as a function of both temperature and doping.
20. E. ABRAHAMS, P. W. ANDERSON, D. C. LICCIARDELLO, AND T. V. RAMAKRISHNAN, *Phys. Rev. Lett.* **42,** 693 (1979).
21. M. A. PAALANEN, J. E. GRAEBNER, R. N. BHATT, AND S. SACHDEV, *Phys. Rev. Lett.* **61,** 597 (1989).
22. C. CASTELLANI, C. DICASTRO, P. A. LEE, AND M. MA, *Phys. Rev. B* **30,** 527 (1984); C. CASTELLANI, G. KOTLIAR, AND P. A. LEE, *Phys. Rev. Lett.* **59,** 323 (1987).